

# Seaweeds in Two Oceans: Beta-diversity

Albertus J. Smit<sup>1,\*</sup>, John J. Bolton<sup>2</sup> and Robert J. Anderson<sup>2,3</sup>

<sup>1</sup>Department of Biodiversity and Conservation Biology, University of the Western Cape, Private Bag X17, Bellville 7535, South Africa

<sup>2</sup>Biological Sciences Department and Marine Research Institute, University of Cape Town, Rondebosch, 7701, South Africa

<sup>3</sup>Seaweed Unit, Fisheries Branch, Department of Agriculture, Forestry and Fisheries, Roggebaai, 8012, South Africa

Correspondence\*:

Albertus J. Smit  
ajsmit@uwc.ac.za

## 2 ABSTRACT

3 Several species assembly mechanisms have been proposed to structure ecological communities. We assess  
4 the biogeography of seaweeds along 2,900 km of South Africa's coastline in relation to a thermal gradient  
5 produced by the Agulhas Current, and contrast this with the environmental structure created by the Benguela  
6 Current. We subdivided the coastline into 'bioregions' to examine the regional patterning. To investigate the  
7 assembly mechanisms, we decomposed Sørensen's  $\beta$ -diversity into 'turnover' ( $\beta_{sim}$ ) and 'nestedness-resultant'  
8 ( $\beta_{sne}$ ) dissimilarities, and used distance-based redundancy analysis (db-RDA) to relate them to the Euclidian  
9 thermal difference,  $d_E$ , and geographical distance. Moran's eigenvector maps (MEM) were used as an additional  
10 set of spatial constraints. Variation partitioning was then used to find the relative strengths of thermal and  
11 spatially-structured thermal drivers. Spatial and environmental predictors explained 97.9% of the total variation  
12 in  $\beta_{sim}$  and the thermal gradient accounted for 84.2% of this combined pool.  $\beta_{sim}$  was the major component  
13 of overall  $\beta$ -diversity in the Agulhas Current region, suggesting niche influences (environmental sorting) as  
14 dominant assembly process there. The much weaker thermal gradient in the Benguela Current-influenced region  
15 resulted in a high amount of  $\beta_{sne}$  that could indicate neutral assembly processes. The intensification of upwelling  
16 during the mid-Pliocene 4.6–3.2 Ma (i.e. historical factors) were likely responsible for setting up the strong  
17 disjunction between the species-poor west coast and species-rich south and east coast floras, and this separation  
18 continues to maintain two systems of community structuring mechanisms in the Atlantic and Indian Ocean  
19 influenced sides of South Africa.

20 Keywords: beta-diversity, species assembly, seaweed, macroalgae, turnover, nestedness-resultant, Benguela Current,  
21 South Africa

## 22 1 Introduction

23 The assembly processes that structure biodiversity across a range of scales form the theme of macroecology  
24 (Chave, 2013). This paper deals with the composition of seaweed assemblages along the ~2,900 km South  
25 African coastline, including the identification, description and explanation for the spatially-structured  
26 patterns at scales from 100s to 1,000s of kilometers. Inshore conditions along this coastline range from  
27 cool through warm temperate to fringe tropical (Bolton and Anderson, 2004; Bolton et al., 2004), and are  
28 influenced by two major ocean currents in two oceans that set up a strong thermal gradient along the shore

29 (Smit et al., 2013). We investigate how a gradient in seaweed community composition may have arisen in  
30 response to this temperature gradient (e.g. Qian and Ricklefs, 2007), and the extent to which deterministic,  
31 niche-based species assembly processes could have contributed towards the assembly of the seaweed flora  
32 of the region.

33 Biodiversity may be viewed in terms of  $\alpha$ -,  $\gamma$ - and  $\beta$ -diversity, with the former two referring to 'local'  
34 and 'regional' diversity, respectively.  $\beta$ -diversity as defined by Whittaker (1960, 1972) is a measure of  
35 variation in species composition from place to place and is comprised of two processes (Baselga, 2012):  
36 the replacement of species independently of the difference in species richness (called 'turnover',  $\beta_{\text{sim}}$ ) and  
37 a term that considers this difference in species richness called ('nestedness-resultant',  $\beta_{\text{sne}}$ ). The relative  
38 contribution of these two processes is not immediately evident from species dissimilarities, and yet such  
39 considerations should be implicit in macroecological studies. The ability to decompose  $\beta$ -diversity into  
40 turnover and nestedness-resultant components has become possible within the last decade (Baselga, 2010),  
41 but the use of this form of  $\beta$ -diversity partitioning has not yet widely permeated the phycological literature  
42 (or even in marine studies more broadly; Anderson et al., 2013). Cognisance of spatial scaling should also  
43 be deeply rooted in the study of biodiversity more generally, but such questions have only recently begun  
44 to be addressed (Barton et al., 2013).

45 Since studies of  $\beta$ -diversity consider the variation in species assembly processes from place to place, and  
46 necessitate an understanding of mechanisms that drive these processes (Davidar et al. 2007), studying  $\beta$ -  
47 diversity of adjacent coastal marine bioregions or marine provinces (Spalding et al., 2007) could provide  
48 deeper insight into how such processes operate along gradients (Qian and Ricklefs, 2007). Few studies  
49 dealing specifically with  $\beta$ -diversity exist for marine biota, especially over spatial areas in excess of 1,000s  
50 of kilometers. Recent examples include studies on fish distribution (Zintzen et al., 2011; Anderson et al.,  
51 2013), the biogeography of macroalgae along 6,600 km of Australian coastline (Leaper et al., 2011), and a  
52 study on deep-sea bivalves (McClain et al., 2011). All four have  $\beta$ -diversity as a primary interest. However,  
53 macroecological studies in the terrestrial realm have yielded the most comprehensive insights into the  
54 drivers responsible for assembling species into communities (Whittaker, 1960; Davidar et al., 2007; Qian  
55 and Ricklefs, 2007; Soininen et al., 2007). What these studies showed is that, perhaps universally, high  
56 rates of species turnover are associated with steep environmental gradients, such as those occurring along  
57 mountain slopes or across latitudes. In the ocean, the biggest driver latitudinally seems to be temperature  
58 (Tittensor et al., 2010; Stuart-Smith et al., 2017; Straub et al., 2016); other drivers such as nutrients, salinity,  
59 turbidity, wave action and photoperiod may also structure species composition, but these are likely to  
60 depend more on the regional context, and some, such as nutrients (e.g. Waldron and Probyn, 1992), are  
61 often strongly correlated with a more distal variable, such as temperature.

62 Recent decades have seen temperature emerging as a readily available environmental driver that's able  
63 to resolve the ocean's heat content across a multitude of temporal and spatial scales. Temperature is also  
64 very useful as a predictor of species range limits due to it being one of the key output variables of coupled  
65 global ocean-atmosphere circulation models used to project the physical milieu of the future Earth that  
66 has experienced anthropogenic climatic change (Church et al., 2013), hence making it the focus of our  
67 present study. The controlling effect of seawater temperature on the survival and reproduction of benthic  
68 organisms and patterns in the evolution and ecology of biological assemblages at regional scales is well  
69 known (van den Hoek, 1982b; Breeman, 1988; Blanchet et al., 2008; Broitman et al., 2008; Byrne et al.,  
70 2009; Verbruggen et al., 2009; Wieters et al., 2009; Couce et al., 2012; Potts et al., 2014). It influences the  
71 species composition of the biota associated with various thermal zones, which forms patterns on global,  
72 regional and local scales (Tittensor et al., 2010; Spalding et al., 2012). At the global scale, ocean currents and

73 well-characterised latitudinal solar heat flux gradients maintain the ocean's thermal regime. At local scales  
74 (<10 km) at the land/sea margin, however, additional less well-known physical phenomena contribute to  
75 thermal patterns and dynamics that may differ markedly from those at the mesoscale (*i.e.* spatial scales  
76 >50 km), and the different properties of the temperature regime which set up the biogeographical patterns  
77 are less well understood there — this is especially true at regional and local scales near the land where  
78 satellite data poorly reflect reality (Smit et al., 2013). Most studies that recognise temperature as a major  
79 driver of species distribution take the annual mean temperature (Tittensor et al., 2010); fewer recognise the  
80 importance of variability and range (*e.g.* Couce et al., 2012; Tyberghein et al., 2012). Detailed laboratory  
81 culture studies with seaweed species, for example, closely link biogeographical distribution limits with  
82 maximum and minimum monthly mean temperatures (van den Hoek, 1982b; Breeman, 1988). The time-  
83 integrated 'thermal environment' is an amalgam of various statistical properties derived from a multitude  
84 of instantaneous temperature recordings, and it is pertinent to question if one or a few of these properties  
85 have an overriding imprint on the species assembly.

86 Understanding the processes influencing species turnover and geographical range is of practical  
87 importance to spatial biodiversity planning. This is especially relevant in today's warming world because  
88 it will allow us to project future biodiversity responses. Focusing conservation efforts on areas of high  
89  $\beta$ -diversity will ensure the preservation of a diversity of species and their environmental niches. Peaks  
90 in  $\beta$ -diversity along ecoclines may indicate boundaries between bioregions, highlighting regions where  
91 communities are poised at their environmental limits, thus aligning with long-term monitoring surveys  
92 that aim to project ecosystem responses to climatic change.

93 Using a detailed data set of seaweed presence and absence records coupled with coastal *in situ* seawater  
94 temperature climatologies that are able to resolve the coastal zone, we investigated the thermal properties  
95 and species composition of 58 coastal sections spaced around the South African coastline. The coastline is  
96 broadly influenced by two major ocean currents, the Benguela Current and the Agulhas Current. One is  
97 an eastern boundary upwelling system and defines a cool temperate environment, and the other a western  
98 boundary current driving meridional transport of sub-tropical water towards the tip of Africa. We were  
99 primarily interested in establishing how these ocean currents, of which the effect at the coast can readily be  
100 measured as gradients in thermal properties, may have influenced the species assembly processes operating  
101 along an approximately 2,900 km long coastline. To do so, we first link matrices of species dissimilarity to  
102 environmental distance matrices and Moran's eigenvector maps (MEM) using distance-based redundancy  
103 analysis, and then apply variance partitioning (Peres-Neto and Legendre, 2010) to determine the relative  
104 contributions of thermal metrics and other spatially-organised drivers of seaweed community composition  
105 (as seen in the  $\beta$ -diversity components,  $\beta_{sim}$  and  $\beta_{sne}$ ). Second, we examine how the thermal and spatial  
106 structuring agents operate at smaller spatial scales within marine provinces of the region by undertaking  
107 a more detailed analysis of the various distance matrices, and also ask which of the thermal properties  
108 we examined were most influential in setting up the patterns that emerged. Our findings are congruent  
109 with existing knowledge (*e.g.* Stephenson, 1948; Lombard et al., 2004; Spalding et al., 2007) and add a  
110 more nuanced understanding of the processes responsible for structuring the seaweed biodiversity in the  
111 sub-region.

## 112 2 Methods

### 113 2.1 Species data and explanatory variables

114 We used three sets of data in this analysis. The first comprises distribution records (presence/absence) of  
115 846 macroalgal species belonging to the Divisions Ochrophyta, Rhodophyta and Chlorophyta within each  
116 of 58 × 50 km-long sections of the South African coast (mentioned in **bold** font in the text and listed in  
117 Appendix A, Table1). The *seaweed data* represent ca. 90% of the known seaweed flora of South Africa in  
118 the intertidal and shallow subtidal, but excludes some very small and/or very rare species for which data  
119 are insufficient. The data are from verifiable literature sources and our own collections, assembled from  
120 information collected by teams of phycologists over three decades (Bolton and Stegenga, 2002; Bolton,  
121 1996, 1986; De Clerck et al., 2005; Stegenga et al., 1997).

122 The second is a dataset of *in situ* coastal seawater temperatures (Smit et al., 2013) derived from daily  
123 measurements over up to 40 years. The *thermal data* set was used as the first set of explanatory variables. The  
124 following statistical properties were entered into the analysis: the means for the year (*annMean*), February  
125 (*febMean*, Austral summer) and August (*augMean*, Austral winter); the annual standard deviation (SD)  
126 around the mean for the year, February and August (*annSD*, *febSD* and *augSD*, respectively); and the annual  
127 thermal range between the mean temperature of the warmest and coldest months (*annRange*), and the  
128 mean range of February and August temperatures (*febRange* and *augRange*).

129 The third set of explanatory variables was generated to represent the spatial connectivity among  
130 coastal sections. Because of the strong environmental gradients along the shore, species community  
131 composition should be spatially organised (including the modelled spatially structured environmental  
132 variables, exogenous spatial variables and autocorrelation), and this was accounted for in the analysis. To  
133 this end we produced a section–section connectivity matrix based on a minimum spanning tree (MST)  
134 topology, starting from a geographical distance matrix. This topology focuses on relationships between  
135 neighbouring sections and discards connections that are further away. In the case of the coastline data,  
136 sections are connected only to other sections that are below a certain truncation distance. This largely  
137 resulted in a ‘string-of-beads’ series of section–section connections; for example, Section 4 is directly  
138 connected to only Sections 3 and 5; sections at the termini of the coastal ‘string’ of sections are each  
139 connected to only one other section. We generated Moran’s eigenvector maps (MEM; Dray et al., 2006,  
140 2012) from this connectivity matrix through a principal coordinates analysis (PCoA) using the PCNM  
141 function of the PCNM package in R 3.3.3 (R Core Team, 2017), and kept the MEMs with positive spatial  
142 correlation. The MEMs are completely orthogonal and represent the spatial structures over the full range  
143 of scales from 50 to 2,900 km. Large eigenvectors represent broad spatial scales while smaller ones cover  
144 finer features. The *spatial data* were used as the second set of explanatory variables in multiple regression  
145 type analyses (Dray et al., 2012). Details and code are provided in Appendix B and may be accessed online  
146 at [https://github.com/ajsmits/Seaweeds\\_in\\_Two\\_Oceans.git](https://github.com/ajsmits/Seaweeds_in_Two_Oceans.git).

### 147 2.2 Distance-based redundancy analysis and variance partitioning

148 Using the distance-based redundancy analysis (db-RDA; Minchin, 1987) implemented with the **capscale**  
149 function of the R package, **vegan** (Oksanen et al., 2016), we explored the role of the thermal and spatial  
150 descriptors in structuring the seaweed communities across the 58 coastal sections. To represent the biotic  
151 data, we decomposed Sørensen’s dissimilarity ( $\beta_{\text{sør}}$ ) into its ‘nestedness-resultant’ ( $\beta_{\text{sne}}$ ) and ‘turnover’  
152 ( $\beta_{\text{sim}}$ ) components (Baselga, 2010) using the **betapart** package (Baselga et al., 2013). This approach was

153 necessary because  $\beta$ -diversity is strongly coupled with  $\alpha$ -diversity, and it allowed us to make inferences  
154 about the possible drivers of  $\beta$ -diversity. Turnover refers to processes that cause communities to differ  
155 due to species being lost and/or gained from section to section, *i.e.* the species composition changes  
156 between sections without corresponding changes in  $\alpha$ -diversity. The nestedness-resultant component  
157 implies processes that cause species to be gained or lost, and the community with the lowest  $\alpha$ -diversity  
158 is a subset of the richer community.

159 The assessment of the biotic ordination within the context of the underlying environmental properties  
160 proceeded using the environmental variables' z-scores. To determine the descriptors that best describe the  
161 patterns in the seaweed dissimilarity data, we first applied full (global) db-RDAs using the complete sets of  
162 thermal and spatial variables, separately for each set. Using the forward selection procedure implemented  
163 in the **packfor** package for R (Blanchet et al., 2008), we reduced the number of variables in each set and  
164 retained only those that best fit the biotic data. Forward selection prevents the inflation of the overall type I  
165 error and reduces the number of explanatory variables used in the final model, which improves parsimony.  
166 The reduced set of thermal variables retained collinear variables (Graham, 2003), which were identified and  
167 removed using variance inflation factors (VIF; Dormann et al., 2013). This was not necessary for the MEMs  
168 as they are orthogonal by definition. The remaining significant orthogonal thermal and spatial variables  
169 were then regressed with  $\beta_{\text{sim}}$  and  $\beta_{\text{sne}}$  and final db-RDA models produced. The computation of db-RDAs  
170 was followed by permutation tests of the adjusted  $R^2$  to assess the significance of constraints (thermal and  
171 spatial descriptors). Lastly we undertook variance partitioning (Peres-Neto et al., 2006; Peres-Neto and  
172 Legendre, 2010) between the environmental (thermal) and spatial predictors using the **varpart** function in  
173 the **vegan** package. Refer to Appendix B for more information about the methodology and for the R code  
174 underlying the analysis.

## 175 2.3 Analyses of dissimilarity and distance matrices

176 We then explored regional patterns in  $\beta$ -diversity. Because connectivity between sections is constrained by  
177 their location along the shore and thus direct distances between sections do not apply, the total distance  
178 between a pair of arbitrary sections is the cumulative sum of the great circle distances between each  
179 consecutive pair of intervening sections along the coast (this is in fact encapsulated by the connectivity  
180 matrix used in the PCNM analysis, above). Plots showing the relationship of  $\beta_{\text{sim}}$  and  $\beta_{\text{sne}}$  with distance  
181 are limited because they do not provide a geographical context. To overcome this problem, we used a  
182 'network graph' to show spatial relationships in regional species dissimilarity. See Appendix C for details  
183 and R code.

184 The last step of our analysis was applied to the four bioregions recognised for South Africa (Bolton and  
185 Anderson, 2004), namely the Benguela Marine Province (BMP; 1–17), the Benguela-Agulhas Transition  
186 Zone (B-ATZ; 18–22), the Agulhas Marine Province (AMP; 19–43/44) and the East Coast Transition Zone  
187 (ECTZ; 44/45–58). To this end, we calculated an Euclidian distance matrix that encapsulated all pairwise  
188 differences between coastal sections for each of the thermal metrics highlighted in the db-RDA (above)  
189 using the **vegan** package; these are called thermal differences ( $d_E$ ) throughout. We then correlated  $\beta_{\text{sim}}$   
190 and  $\beta_{\text{sne}}$  with geographical distance and  $d_E$  and provided matching plots in which the four bioregions were  
191 colour-coded to discern bioregional affiliations and differences. Together these analyses were able to capture  
192  $\beta$ -diversity at two spatial scales: among sections within bioregions, and among all sections for the whole  
193 country.

### 194 3 Results

#### 195 3.1 The thermal environment and species richness

196 South Africa's annual mean coastal water temperature ranged from  $12.0 \pm 0.9^\circ\text{C}$  (mean  $\pm$  SD) at its north-  
197 western limit near the Namibian border (1) to  $24.0 \pm 1.9^\circ\text{C}$  on the east coast near the Mozambican border  
198 (58) (Fig. 1). The global latitudinal gradient of diminishing temperature with increasing latitude was seen  
199 only along the east coast where the annual mean temperature decreased from *ca.*  $24.5^\circ\text{C}$  near 58 to  $17.5^\circ\text{C}$   
200 around 39. The alongshore thermal gradient for this 950 km stretch of coastline was *ca.*  $0.7^\circ\text{C}$  per 100 km,  
201 with steeper gradients near 54. The latitudinal gradient largely reversed in direction along the west coast  
202 (1–16), *i.e.* temperatures became slightly cooler further north.

203 **Figure 1 near here.**

204 On average, these data indicated an increase in inshore annual mean temperatures from west to east  
205 (1–58) of  $12.1\text{--}24.4^\circ\text{C}$  (range:  $12.3^\circ\text{C}$ ). In February the thermal range was  $13.7^\circ\text{C}$ , while in August it was  
206  $10.5^\circ\text{C}$ . In August the west–east temperature transition was smooth whereas in February substantial warm  
207 fluctuations in the mean monthly temperature were observed in embayments such as 13 and the False Bay  
208 sections from 17–18, and 28 and some sections around 35/36 and Algoa Bay from 34–36. In summer the  
209 mean monthly temperature gradient steepened between 19–28, and thereafter decreased eastwards along  
210 the coast from 33–34.

211 The number of species within the BMP was low, and many northern sections had fewer than 150 species,  
212 and it rose significantly in the warmer section around 12/13, and the southern sections around the Cape  
213 Peninsula (16/17). Thereafter, richness increased markedly in the B-ATZ, the AMP and the ECTZ. The  
214 highest number of species in any one section was 340 (Section 39 near the eastern end of the AMP).

#### 215 3.2 Environmental correlates of seaweed diversity

216 db-RDA, forward selection and the assessment of VIF retained *augMean*, *febRange*, *febSD* and *augSD* as  
217 the most parsimonious descriptors of  $\beta_{\text{sim}}$  with an adjusted  $R^2$  of 0.885, explaining 89.8% of the variation  
218 (global permutation test on final model: d.f. = 4,  $F = 110.16$ ,  $p = 0.001$ ). The model consisted of two  
219 significant canonical axes: CAP1 and CAP2 explained 73.3% and 14.9% of the variation, respectively. The  
220 biplot scores (vectors) showed that *augMean* was heavily loaded along CAP1 and the metrics related to  
221 variation around the mean, *i.e.* *febRange* and *febSD*, strongly influenced  $\beta_{\text{sim}}$  along CAP2 (Fig. 2). Plots  
222 of the 'lc' scores on geographic axes are given in Fig. 3. The scores representing CAP1 increased gradually  
223 along the shore from west to east, reflecting the pervasive influence of *augMean* as coastal sections changed  
224 from cool to warm temperate through to sub-tropical thermal regimes. CAP2 site scores were lowest along  
225 the southern sections.  $\beta_{\text{sne}}$  was only influenced by *annMean* (Fig. 2) along CAP1 that explained 20.3% of  
226 the total variation ( $R^2 = -0.140$ , d.f. = 1,  $F = -6.018$ ).

227 **Figure 2 near here.**

228 The db-RDA analysis procedure retained 17 significant MEMs that fully encapsulated the spatial  
229 dependence within  $\beta_{\text{sim}}$  (d.f. = 18,  $F = 84.055$ ,  $p = 0.001$ ), resulting in an adjusted  $R^2$  of 0.963 and accounting  
230 for all of the variation. Fifteen canonical axes were produced of which five were significant. The first one  
231 alone explained 77.1% of variance with the remaining axes accounting for *ca.* 1% or less of the inertia.  
232 MEM2, MEM3 and MEM5 were most strongly loaded along CAP1 (Fig. 3). These MEMs caused the  
233 sections belonging with the BMP to separate out from all other sections, and also for the northern sites

of the ECTZ to diverge from the sections and bioregions further south. The scales of spatial dependence captured by these MEMs could all be considered to be broad-scaled. Two canonical axes comprised of two significant MEMs were able to explain 87.3% of the variation in  $\beta_{\text{sne}}$  ( $R^2$  of 0.437, d.f. = 4,  $F = 12.06$ ,  $p = 0.001$ ; Fig. 3). CAP1 consumed 79.0% of the inertia due to MEM1 and MEM5.

**Figure 3 near here.**

The partitioning of the variance associated with the seaweed community along the coast (Table 1) was explained jointly by the thermal and spatial variables selected in the preceding db-RDAs. Combining the thermal and spatial predictors (fractions [E+S]) allowed the model to capture 97.9% of the total  $\beta_{\text{sim}}$  variance ( $F = 191.56$ ,  $p = 0.001$ ), with a residual variance of 2.1%. The thermal variables on their own (*i.e.* those that are spatially unstructured; fraction [E|S]) were able to account for only 1.8% of the total variation ( $F = 20.506$ ,  $p = 0.001$ ), but including some spatially structured thermal properties, [E], raised the proportion of explained variation to 84.2% ( $F = 110.16$ ,  $p = 0.001$ ). Pure spatial patterning (*i.e.* in the absence of temperature influences, perhaps with exogenous environmental influences or autocorrelation; fraction [S|E]) drove 13.7% of the species variation ( $F = 23.649$ ,  $p = 0.001$ ), and adding some thermal influences together with spatial descriptors, [S], increased this to 96.1% ( $F = 80.731$ ,  $p = 0.001$ ). Turning now to  $\beta_{\text{sne}}$ , we see that our explanatory variables were less successful in capturing the variation. The spatial variables, [S], and the spatial plus thermal variables, [E+S], were able to account for 67.8% ( $F = 12.06$ ,  $p = 0.001$ ) and 71.4% ( $F = 9.077$ ,  $p = 0.001$ ) of the variation, respectively.

**Table 1 near here.**

### 3.3 Pairwise dissimilarities

Network graphs show the spatial relationships of  $\beta_{\text{sim}}$  (Fig. 4).  $\beta_{\text{sim}}$  clearly highlighted the effect of the sharp change in  $\alpha$ -diversity between the BMP and the B-ATZ. Sections in the B-ATZ retained similarities with sections as far east as 33 within the AMP. Eastwards from 30 similarities with sections within the ECTZ became apparent, but they generally did not extend past 43. Aside from a very low similarity with sections at the eastern extent of the AMP, the ECTZ sections retained similarities with sections within the same biogeographical province only over very short distances, and again it highlighted the high  $\beta$ -diversity in this region.

**Figure 4 near here.**

The overall and regional mean values for the three measures of pairwise  $\beta$ -diversity are presented in Table 2. The overall Sørensen  $\beta$ -diversity ( $\beta_{\text{sør}}$ ,  $0.496 \pm 0.287$ ) was larger than that of the bioregions, and only a small fraction of it was comprised of nestedness-resultant  $\beta$ -diversity. Of the four bioregions, the ECTZ had the highest  $\beta_{\text{sør}}$  ( $0.259 \pm 0.157$ ). At the bioregional scale, it is important to note that the nestedness-resultant component was about four times larger for the BMP ( $\beta_{\text{sne}}/\beta_{\text{sør}} = 0.581$ ) than that of the other three ( $\beta_{\text{sne}}/\beta_{\text{sør}}$  ranged from 0.097 to 0.170).

Plots of  $\beta_{\text{sim}}$  and  $\beta_{\text{sne}}$  among all possible section pairs indicated clear differences among the four bioregions in their relationships with geographic and thermal distances (Fig. 5). The BMP showed a weak relationship between  $\beta_{\text{sim}}$  and distance ( $r^2 = 0.052$ ; regression statistics in Table 3) since much of the compositional variation between sections in this region was due as much to nestedness-resultant  $\beta$ -diversity as it was to turnover (Fig. 5) as noted above (see  $\beta_{\text{sne}}/\beta_{\text{sør}}$  in Table 2). Within the ECTZ (~900 km long coastline) and the B-ATZ (only 170 km long) the rates were moderate at  $\beta = 0.079$  ( $r^2 = 0.936$ ) and high at  $\beta = 0.109$  ( $r^2 = 0.658$ ) per 100 km, respectively. In the AMP it was lower at  $\beta = 0.029$

per 100 km ( $r^2 = 0.834$ ). Higher rates ( $\beta$ ) indicate that communities turned over more rapidly per unit distance of coastline; furthermore, this also provided strong evidence that  $\beta$ -diversity was structured along environmental gradients.  $\beta$ -diversity was less influenced by changes in species numbers between sections in the B-ATZ, AMP and the ECTZ, as these two marine provinces were characterised by a relatively even number of species and hence had low  $\beta$ -diversities attributed to nestedness (Fig. 5).  $\beta_{\text{sim}}$  expressed with respect to the *augMean* thermal distance showed similarly steep slopes for three of the bioregions ( $\beta$ s ranging from 0.290 to 0.350, with  $r^2 > 0.605$ ), with that for the BMP about a two-thirds lower (Fig. 5; Table 3). With respect to *febRange*, a significant relationship with  $\beta_{\text{sim}}$  existed only for the two transitional areas, the B-ATZ and the ECTZ ( $r^2$  of 0.548 and 0.583, respectively; Fig. 5). The steepness of the relationship between  $\beta_{\text{sim}}$  and the latter thermal metric was lower than that seen with *augMean*. Concerning *febSD*, this relationship was steepest for the B-ATZ ( $\beta = 0.103$ ,  $r^2 = 0.276$ ) and then the ECTZ ( $\beta = 0.082$ ,  $r^2 = 0.310$ ; Fig. 5); the same general trend held for *augSD*, with  $r^2 = 0.310$  and  $r^2 = 0.276$  for the ECTZ and B-ATZ, respectively. The pattern of  $\beta_{\text{sne}}$  with geographic and thermal distance was generally significant but very poor (low  $r^2$ -values) and with weak gradients ( $\beta$ ) (Fig. 5). The notable outcome there was that it was the BMP where  $\beta_{\text{sne}}$  was strongest even though its  $r^2$  values were weak ( $r^2 = 0.205$  and 0.164 for the relationship with geographical distance and thermal distance, respectively).

Figure 5 near here.

Table 2 near here.

Table 3 near here.

## 4 Discussion

This study considered the drivers of seaweed  $\beta$ -diversity at the scale of bioregions (marine provinces) nested within a ~2,900 km stretch of coastline. With the exception of the some Australian studies (Smale et al., 2010, 2011; Waters et al., 2010; Leaper et al., 2011; Wernberg et al., 2013), one in Europe (Tuya et al., 2012) and another two in the Arabian region (Schils and Wilson, 2006; Issa et al., 2016), studies of this scale and nature have so far been infrequently seen for marine macroalgae. Of the above-mentioned studies, only two specifically considered  $\beta$ -diversity (Leaper et al., 2011; Issa et al., 2016). Our data focus on the taxonomic representativity of a region by aggregating species occurrence records within 50 km long sections of coastline, and are blind to the effects of small-scale habitat heterogeneity (e.g. as seen in Smale et al., 2010). For this reason we cannot infer influences of stochastic processes and other aspects of environmental heterogeneity at scales of <50 km; as such we excluded drivers that may be only of local relevance, such as salinity, turbidity (light), and wave action. Rather, our data emphasise broad biogeographic patterns (Lawton, 1999), with induced spatial dependence (Peres-Neto and Legendre, 2010) emerging as the main species assembly process east of the Cape Peninsula. This points to deterministic niche influences that correlate with environmental drivers that function over a broad spatial scale. These environmental and biotic patterns reflect the nature of the two dominant ocean currents of the region, and we see that  $\beta$ -diversity at the scale of the country is moderately high and generally influenced by processes that cause species turnover ( $\beta_{\text{sim}}$ ). Our selected environmental drivers comprise mostly thermal properties of seawater with a strong spatial dependence across a broad scale (82.4%) and a smaller amount of unknown non-thermal broad-scale spatial influences (13.7%). Only in the species-poor west coast region is there evidence of neutral assembly processes (e.g. dispersal limitation, and stochastic processes as one might expect within kelp forests), as shown by the higher rates of nestedness-resultant  $\beta$ -diversity ( $\beta_{\text{sne}}$ ) emerging there. We recognise that some environmental drivers such as nutrients can and do co-vary with temperature, but

317 they were not used in our analysis because they are not as readily measured as temperature, they are not  
318 always directly produced by coupled global ocean-atmosphere models and thus have less value as predictive  
319 (long-term) variables, and because of the issues arising due to collinearity.

320 The most comprehensive assessment of global marine biogeography (Spalding et al., 2007) places much  
321 of South Africa's coast within two realms: Temperate Southern Africa (from southern Angola to around  
322 56°) and the western-most edge of the Western Indo-Pacific Realm (across the Western Indian Ocean to  
323 Sumatra). The transition into the Western Indian Ocean realm is just visible in Section 57 where our data  
324 show a steady rise to tropical water temperatures that exceed 20°C, between 28.5 and 29°S. Our study region  
325 is too restricted to capture the rates of  $\beta$ -diversity change at the transition of realms. Here we would expect  
326 higher rates of turnover than we report for the smaller-scale 'Provinces' and transition zones that make up  
327 the Temperate Southern African Realm (see below). We would also expect this at higher taxonomic levels,  
328 consistent with the definition for a realm (Spalding et al., 2007): this is true for the temperate Southern  
329 African seaweed floras, which have high species endemism but very low generic endemism (except for the  
330 Fucales, Ochrophyta). We hypothesise that this is because the cool temperate region may be geologically  
331 recent (4.6–3.2 Ma, Marlow et al., 2000).

332 Nested within the realms are marine provinces, areas that according to (Spalding et al., 2007) are large,  
333 with distinct biotas, some level of endemism (mainly at species level), and distinctive abiotic environments.  
334 In this context, the Benguela and Agulhas Currents prescribe the broadest scale hydrographic features  
335 whose imprint can be seen, at that scale, on the seaweed flora: they maintain the Benguela Marine Province  
336 (BMP) and Agulhas Marine Province (AMP, as per Spalding et al., 2007) of South Africa, separated  
337 by an area of transition. The southward flowing Agulhas Current has an overriding effect on the east  
338 coast, extending as far as the eastern portion of the Western Cape Province (58–22). Along the east  
339 coast it is responsible for setting up a region that transitions from sub-tropical in the north to warm  
340 temperate near Cwebe (*i.e.* the region 58–44), which is termed the East Coast Transition Zone (ECTZ).  
341 From 44–22 the Agulhas Current continues to maintain an influence on the coast, but its direct effect is  
342 subdued because of the widening of the continental shelf southwards of Cwebe, and the warm-temperate  
343 biogeographical region, the AMP, is consequentially formed. The northward flowing Benguela Current  
344 from which upwelling is maintained by prevailing south-easterly trade winds influences the remainder of  
345 the Western Cape Province (west of 22), particularly from the western side of the Cape Peninsula (16/17)  
346 northwards to about 16°S. The influence of the Benguela Current here defines a cool-temperate regime, the  
347 BMP, with the range of monthly mean temperatures at most sections intermediate between cold-temperate  
348 and warm-temperate, according to the definitions of (Lüning et al., 1990).

349 The oceanographic features of the Benguela and Agulhas Currents set up gradients in seawater  
350 temperature that run predominantly from east to west (*i.e.* August mean temperatures increasing in this  
351 direction), but also from north to south (*i.e.* with the southern coastline becoming more variable in its  
352 thermal regime). Of particular ecological importance is the gradient in August mean temperature. It clearly  
353 structures the thermal distance decay curve, which shows a steadily increasing dissimilarity in thermal  
354 distance along the shore from 1. The gradient may be smooth or punctuated at irregular intervals by  
355 peaks in dissimilarity. Specifically, the mean temperature for Austral winter (August) increases more-or-  
356 less smoothly from the west. Within the region, species richness along the coastline reflects the general  
357 global trend — for most taxa but ironically not for seaweeds (Bolton, 1994; Santelices et al., 2009) — of  
358 diminishing diversity with decreasing temperature, which at that scale is seen as a latitudinal gradient:  
359 the cold temperate area of the west coast has a much lower  $\alpha$ -diversity than the warm temperate and sub-  
360 tropical south and east coasts, with the latter two regions having similar values. This same pattern exists

361 for fish and invertebrates in this region, albeit in data which include coastal waters further from the shore  
362 (Griffiths et al., 2010). In the previous presentation of the seaweed dataset (Bolton and Stegenga, 2002), the  
363 ECTZ had far fewer species per section than the AMP, but this change in the dataset results from significant  
364 research in the period 2000–2005 on the seaweeds of the ECTZ (De Clerck et al., 2005). In contrast, bringing  
365 the annual mean temperature or thermal range during Austral summer into the calculation of the thermal  
366 distance introduces several large punctuations in dissimilarities between some sections — most notably  
367 near Cape Point into False Bay (17), and near 30 and 48. The region of the coastline where low biodiversity  
368 community composition changes to highly biodiverse communities is reflected in the  $\beta$ -diversity, which  
369 peaks around the Cape Peninsula (16/17). Correlations between  $\beta$ -diversity (resulting from a change in  
370  $\alpha$ -diversity) and areas of transition have also been noted in several studies on terrestrial biota (Melo et al.,  
371 2009; Tonial et al., 2012), but such investigations are less established for marine biota (Schils and Wilson,  
372 2006; Anderson et al., 2013).

373  $\beta$ -diversity is generally lower within individual bioregions than at the scale of the country, because the  
374 coastlines are shorter and large differences in diversity cannot approach that which can occur over the entire  
375 coastline. Even within bioregions,  $\beta$ -diversity is still *generally* dominated by species turnover rather than  
376 by nestedness-resultant processes. The exception is the BMP where nestedness-resultant ( $\beta_{sne}$ ) assembly  
377 processes contribute to around 58% of the  $\beta$ -diversity. The generally strong influence of turnover-based  
378 processes elsewhere highlights the role of environmental drivers, which here are spatially structured as  
379 one would expect of the steep environmental gradients, and hence of niche influences (*i.e.* environmental  
380 filtering) in determining species assembly (Fitzpatrick et al., 2013).

381 It seems plausible that factors linked with the establishment of oceanographic regimes (historical  
382 factors *sensu* Baselga et al., 2012) that influenced dispersal and speciation along the coast resulted in  
383 the current-day gradients in  $\beta$ -diversity within bioregions. This hypothesis was put forward to explain  
384 the low endemism and low species richness of Ochrophyta in the upwelling dominated west coast of  
385 southern Africa (Bolton, 1986). But is the underlying mechanism the selection of cold tolerant species  
386 from amongst a more diverse pool in the wider region (Bolton, 1986), or is it due to a dispersal barrier  
387 that prevented elements of the warmer south coast seaweed flora from occupying the west coast? Evidence  
388 from seaweed phylogeography postulates different evolutionary origins for seaweeds of the BMP and AMP  
389 (Hommersand, 1986; Hommersand and Fredericq, 2003). The mechanism could be the intensification of  
390 upwelling during the mid-Pliocene 4.6–3.2 Ma (Marlow et al., 2000). Turnover is almost entirely absent  
391 in favour of nestedness-resultant processes in the BMP, but the AMP is defined entirely by a moderate  
392 rate of turnover with respect to both geographical and thermal distance. The dominance of the nestedness-  
393 resultant component of  $\beta$ -diversity within the BMP suggests that the complex, non-linear influence of the  
394 annual mean temperature selectively influences species richness from section to section in a pattern that is  
395 not spatially coherent, but this climatic variable (*i.e.* fraction [E], which has *some* spatial structure) explains  
396 only 39.1% of the  $\beta_{sne}$  patterning in the region. Unaccounted-for non-climatic variables and perhaps  
397 non-environmental variables may explain some of the remaining variation. This points to habitat and/or  
398 environmental heterogeneity and neutral processes such as dispersal limitation, stochastic influences or  
399 habitat heterogeneity as the main structuring agents of communities within the region. Indeed, habitat  
400 heterogeneity generated through stochastic influences such as patchiness due to storms denuding portions  
401 of kelp beds (which is the dominant habitat type along the west coast) is well-known in kelp forests (Smale  
402 et al., 2011). Furthermore, the prevalence of two kinds of assembly processes to either side of the Cape  
403 Peninsula (17), coinciding with the point where a region of low  $\alpha$ -diversity (BMP) transitions into a region  
404 of higher  $\alpha$ -diversity (the Benguela-Agulhas Transition Zone, B-ATZ), suggests that the answer to our  
405 question is probably that some historical event was responsible for that disjunction, and that this barrier is

406 still maintained today due to limited mixing between the Agulhas and Benguela Currents (although some  
407 of the sections along the west coast between 16/17 and 10 certainly have a reasonable probability of sharing  
408 species with sections at the western-most side of the AMP, e.g. 23, 24; see more on the B-ATZ, below).

409 Rapid rates of species turnover with respect to geographic and thermal distance along the east coast,  
410 and the steep decrease in species richness around the 16/17–22 transition region, suggest that relatively  
411 more endemic species should occur within the BMP and AMP. Seawater becomes warmer along a steep  
412 gradient along the east coast northward towards 54 where-after there is a further steepening of the gradient  
413 towards Mozambique (north of 58). This steepening of the already strong temperature gradient in the  
414 northern portion of the ECTZ supports the conclusion of (Bolton and Anderson, 2004) that it represents  
415 the transition from a tropical Indian Ocean seaweed flora in Mozambique to a temperate flora in the south.  
416 A similar pattern exists for the rocky intertidal biota in the region (Sink et al., 2005). The temperature of  
417 the coldest month of the year sufficiently accounts for the environmental gradient in all bioregions, except  
418 for in the BMP. This strong coupling between the thermal gradient and  $\beta_{\text{sim}}$  suggests that a niche difference  
419 mechanism is the primary species compositional assembly process (Nekola et al., 1999). This implies species  
420 being sorted based on their physiological tolerances along a gradient, and the particularly high rate of  
421 species turnover along the east coast reflects the species' narrow thermal ranges. Species here have narrow  
422 local distributions, and there is only a 2% seaweed endemism in the region (Bolton and Anderson, 2004).

423 The overlap region between 22 and the southern tip of the Cape Peninsula (16/17), which we call the  
424 B-ATZ, is an area where aspects of both currents may be periodically seen (Largier et al., 1992), and it  
425 is not surprising that biogeographically this region includes biotic elements from the marine provinces  
426 on both sides of it. This is clearly visible in our analyses, which show the highest rates of species turnover  
427 ( $\beta_{\text{sim}}$ ) with respect to geographical distance, the mean temperature for August and the range in temperature  
428 in February. This is a form of regional biogeographical structuring called the temporal/spatial constraint  
429 model (Nekola et al., 1999). Similar conclusions with regards to the B-ATZ being an transitional area have  
430 been reached by (Stephenson, 1948; Bolton, 1986; Bolton and Anderson, 2004; Mead et al., 2013). For  
431 marine macroalgae at least, this area cannot be recognised as a marine province as it does not meet the  
432 criteria for it to be classified as such (Spalding et al., 2007), i.e. it lacks cohesion, levels of endemism, and  
433 there is an absence of distinct abiotic features (with exception of such conditions periodically arising in  
434 False Bay due to prevailing mesoscale oceanographic conditions).

435 It was recently suggested that studies which associate marine macroalgal distributional patterns with  
436 broad-scale temperature gradients neglect to consider alternative or additional explanations, such as that  
437 offered by connectivity due to ocean currents (Wernberg et al., 2013). It is possible that seaweeds are  
438 similarly influenced by ocean currents around South Africa, and it is tempting to suggest that the *direction*  
439 of turnover along the east coast is from north to south, and along the south coast from east to west, as this  
440 would coincide with the direction of the Agulhas Current. From a purely thermal point of view, the imprints  
441 of those ocean currents are certainly present at the coast in the zone that our seaweed data represent, but  
442 the physical processes that operate in that coastal zone are considerably more complex and decoupled from  
443 mesoscale influences (Schlegel et al., 2017). Personal observations by one of us (AS) recount dislodged  
444 individuals of the kelp, *Ecklonia maxima*, having washed ashore some 400 km east of the eastern-most  
445 distributional limit for the species in South Africa — this is *against* the direction of the current, which  
446 in this region is situated considerably far from the shore along the edge of the Agulhas Bank. Our data  
447 on the rate of species turnover as a function of the thermal difference between coastal sections ( $\beta_{\text{sim}}$   
448 vs.  $d_E$ ) within bioregions show an almost precise relationship between thermal difference and change in  
449 species composition (even though the relationship between  $d_E$  and geographical distance differs between

450 the east and south coasts), and provide very strong support for temperature, rather than connectivity due  
451 to currents, as an overriding driver of seaweed community composition over large spatial scales. Within  
452 the context of Beijerinck's 'Law' that "everything is everywhere but the environment selects" (De Wit and  
453 Bouvier, 2006), the only role that ocean currents can have in setting up biogeographical patterns is to  
454 cause *everything not to be everywhere*. At these scales, with or without the influence of ocean currents,  
455 temperature still selects. In other words, at broad spatial scales within the region encompassed by the  
456 ECTZ and the AMP, the seaweed flora is structured predominantly by niche-assembly processes driven  
457 by a thermal gradient.

458 However, we should point out that *ca.* 13.7% of the seaweed flora's turnover is also explained by  
459 some other broad scale spatial influences (MEM2, MEM3 and MEM5), which represent exogenous  
460 (unmeasured) environmental variables and autocorrelation. The importance of these relative to each other  
461 is unknown. Future work may find that some of these environmental influences may indeed be that of  
462 ocean currents, which operate at those broad scales, but our current interpretation does not support this  
463 notion. Rather, we suggest that the unknown influence is more likely to be neutral influences (Hubbell,  
464 2001) manifesting at a reasonably broad scale. These may include stochastic events (e.g. Smale et al., 2011)  
465 or biotic processes caused by differences in species demography, dispersal or the influence of grazers, etc.  
466 Such processes are usually finer scaled, but, having said that, the entire west coast region that makes up  
467 the BMP is dominated by nestedness-resultant  $\beta$ -diversity, which is also symptomatic of neutral assembly  
468 processes.

#### 469 4.1 Conclusions

470 Our approach throughout this paper hinges upon the biogeographical provinces and overlap regions  
471 defined using both seaweed and thermal data. Together, thermal and species gradients/patterns provide  
472 the most parsimonious explanation for the processes assembling the seaweed flora within the study region.  
473 The explanation is that thermal gradients set up  $\beta$ -diversity based on species turnover as a result of  
474 environmental filtering within the southern and eastern coastal sections, while along the west coast a  
475 very different kind of assembly process, nestedness-resultant  $\beta$ -diversity, emerges. We suggest that this  
476 disjunction results from a historical event that is currently still limiting connectivity between the Indian  
477 and Atlantic Oceans around the Cape Peninsula.

478 We also show how thermal metrics other than the annual mean temperatures can aid in the delineation  
479 of macroecological patterns. Some species are limited by cold and some by warm temperatures, and  
480 the constraining factor may differ at a species' southern and northern limits (e.g. van den Hoek, 1982a;  
481 Breeman, 1988). If these are important determinants, as we indeed show there are, other measures of  
482 climate should be used in our repertoire of explanatory variables. For example, the mean temperature for  
483 the coldest month, standard deviation, variation in annual temperature extremes, or temperature ranges  
484 (e.g. as used by Qian and Ricklefs, 2007; Leaper et al., 2011) may readily be extracted from time series of  
485 daily temperatures. These approaches, as we apply them here, may greatly improve macroecological and  
486 biogeographic studies and aid our ability to analyse broad-scale communities patterns and the processes  
487 that assemble them.

#### 488 Conflict of Interest Statement

489 The authors declare that the research was conducted in the absence of any commercial or financial  
490 relationships that could be construed as a potential conflict of interest.

## 491 Author Contributions

492 AS conceptualised the scope of the research reported in this paper, undertook all the numerical and  
493 statistical analyses, made the first round of interpretation, and did the bulk of the writing. JB and RA  
494 collected all the samples over the last 30 years, compiled the database of species distribution records for the  
495 region included in this analysis, contributed in equal part to the conceptualisation of the research and the  
496 interpretation of the findings, and provided significant editorial input into penultimate and final drafts of  
497 the document.

## 498 Funding

499 The research was partly funded by the South African National Research Foundation (<http://www.nrf.ac.za>)  
500 programme “Thermal characteristics of the South African nearshore: implications for biodiversity”  
501 (CPRR14072378735).

502 Aside from providing funding, the funders had no role in the study design, data collection and analysis,  
503 decision to publish, or preparation of the manuscript.

## 504 Acknowledgments

505 Robert Schlegel is thanked for his assistance in the preparation of some of Figure 1.

## 506 References

- 507 Anderson, M. J., Tolimieri, N., and Millar, R. B. (2013). Beta diversity of demersal fish assemblages in the  
508 North-Eastern Pacific: interactions of latitude and depth. *PLOS ONE* 8, e57918
- 509 Barton, P. S., Cunningham, S. A., Manning, A. D., Gibb, H., Lindenmayer, D. B., and Didham, R. K. (2013).  
510 The spatial scaling of beta diversity. *Global Ecology and Biogeography* 22, 639–647
- 511 Baselga, A. (2010). Partitioning the turnover and nestedness components of beta diversity. *Global Ecology  
512 and Biogeography* 19, 134–143
- 513 Baselga, A. (2012). The relationship between species replacement, dissimilarity derived from nestedness,  
514 and nestedness. *Global Ecology and Biogeography* 21, 1223–1232
- 515 Baselga, A., Gómez Rodríguez, C., and Lobo, J. M. (2012). Historical legacies in world amphibian  
516 diversity revealed by the turnover and nestedness components of beta diversity. *PLOS ONE* 7, e32341
- 517 Baselga, A., Orme, D., Villeger, S., Bortoli, J. D., and Leprieur, F. (2013). *betapart: Partitioning beta diversity  
518 into turnover and nestedness components*. R package version 1.3
- 519 Blanchet, F. G., Legendre, P., and Borcard, D. (2008). Forward selection of explanatory variables. *Ecology*  
520 89, 2623–2632
- 521 Bolton, J. (1994). Global seaweed diversity: patterns and anomalies. *Botanica Marina* 37, 241–246
- 522 Bolton, J. J. (1986). Marine phytogeography of the Benguela upwelling region on the west coast of southern  
523 Africa: A temperature dependent approach. *Botanica Marina* 29, 251–256
- 524 Bolton, J. J. (1996). Patterns of species diversity and endemism in comparable temperate brown algal floras.  
525 *Hydrobiologia* 326–327, 173–178
- 526 Bolton, J. J. and Anderson, R. J. (2004). Marine Vegetation. In *Vegetation of Southern Africa*, eds. R. M.  
527 Cowling, D. M. Richardson, and S. M. Pierce (Cambridge University Press). 348–370

- 528 Bolton, J. J., Leliaert, F., De Clerck, O., Anderson, R. J., Stegenga, H., Engledow, H. E., et al. (2004).  
529 Where is the western limit of the tropical Indian Ocean seaweed flora? An analysis of intertidal seaweed  
530 biogeography on the east coast of South Africa. *Marine Biology* 144, 51–59
- 531 Bolton, J. J. and Stegenga, H. (2002). Seaweed species diversity in South Africa. *South African Journal of*  
532 *Marine Science* 24, 9–18
- 533 Breeman, A. M. (1988). Relative importance of temperature and other factors in determining geographic  
534 boundaries of seaweeds: experimental and phenological evidence. *Helgoländer Meeresuntersuchungen*  
535 42, 199–241
- 536 Broitman, B. R., Blanchette, C. A., Menge, B. A., Lubchenco, J., Krenz, C., Foley, M., et al. (2008). Spatial  
537 and temporal patterns of invertebrate recruitment along the west coast of the United States. *Ecological*  
538 *Monographs* 78, 403–421
- 539 Byrne, M., Ho, M., Selvakumaraswamy, P., Nguyen, H. D., Dworjanyn, S. A., and Davis, A. R. (2009).  
540 Temperature, but not pH, compromises sea urchin fertilization and early development under near-future  
541 climate change scenarios. *Proceedings of the Royal Society B: Biological Sciences* 276, 1883–1888
- 542 Chave, J. (2013). The problem of pattern and scale in ecology: what have we learned in 20 years? *Ecology*  
543 *Letters* 16 Suppl 1, 4–16
- 544 Church, J. A., Clark, P. U., Cazenave, A., Gregory, J. M., Jevrejeva, S., Levermann, A., et al. (2013). Climate  
545 change 2013: the physical science basis. contribution of working group i to the fifth assessment report of  
546 the intergovernmental panel on climate change. *Sea level change*, 1137–1216
- 547 Couce, E., Ridgwell, A., and Hendy, E. J. (2012). Environmental controls on the global distribution of  
548 shallow-water coral reefs. *Journal of Biogeography* 39, 1508–1523
- 549 Davidar, P., Rajagopal, B., Mohandass, D., Puyravaud, J.-P., Condit, R., Wright, S., et al. (2007). The effect  
550 of climatic gradients, topographic variation and species traits on the beta diversity of rain forest trees.  
551 *Global Ecology and Biogeography* 16, 510–518
- 552 De Clerck, O., Bolton, J. J., Anderson, R. J., and Coppejans, E. (2005). Guide to the seaweeds of KwaZulu-  
553 Natal. *Scripta Botanica Belgica* 33, 294 pp.
- 554 De Wit, R. and Bouvier, T. (2006). 'Everything is everywhere, but, the environment selects'; what did Baas  
555 Becking and Beijerinck really say? *Environmental Microbiology* 8, 755–758
- 556 Dormann, C. F., Elith, J., Bacher, S., Buchmann, C., Carl, G., Carré, G., et al. (2013). Collinearity: a review  
557 of methods to deal with it and a simulation study evaluating their performance. *Ecography* 36, 027–046
- 558 Dray, S., Legendre, P., and Peres-Neto, P. R. (2006). Spatial modelling: a comprehensive framework for  
559 principal coordinate analysis of neighbour matrices (PCNM). *Ecological Modelling* 196, 483–493
- 560 Dray, S., Pélassier, R., Couturon, P., Fortin, M. J., Legendre, P., Peres-Neto, P. R., et al. (2012). Community  
561 ecology in the age of multivariate multiscale spatial analysis. *Ecological Monographs* 82, 257–275
- 562 Fitzpatrick, M. C., Sanders, N. J., Normand, S., Svenning, J.-C., Ferrier, S., Gove, A. D., et al. (2013).  
563 Environmental and historical imprints on beta diversity: insights from variation in rates of species  
564 turnover along gradients. *Proceedings of the Royal Society B: Biological Sciences* 280, 20131201
- 565 Graham, M. H. (2003). Confronting multicollinearity in ecological multiple regression. *Ecology* 84, 2809–  
566 2815
- 567 Griffiths, C. L., Robinson, T. B., Lange, L., and Mead, A. (2010). Marine biodiversity in South Africa: an  
568 evaluation of current states of knowledge. *PLOS ONE* 5, e12008
- 569 Hommersand, M. (1986). The biogeography of the South African marine red algae: A model. *Botanica*  
570 *Marina* 29, 257–270
- 571 Hommersand, M. H. and Fredericq, S. (2003). Biogeography of the marine red algae of the South African  
572 West Coast: a molecular approach. *Proceedings of the International Seaweed Symposium* 17, 325–336

- 573 Hubbell, S. P. (2001). The unified neutral theory of biodiversity and biogeography. *Monographs in*  
574 *Population Biology*
- 575 Issa, A. A., Hifney, A. F., Abdel-Gawad, K. M., and Gomaa, M. (2016). Spatio temporal and environmental  
576 factors influencing macroalgal  $\beta$  diversity in the Red Sea, Egypt. *Botanica Marina* 57, 1–13
- 577 Largier, J. L., Chapman, P., Peterson, W. T., and Swart, V. P. (1992). The western Agulhas Bank: circulation,  
578 stratification and ecology. *South African Journal of Marine Science* 12, 319–339
- 579 Lawton, J. H. (1999). Are there general laws in ecology? *Oikos* 84, 177
- 580 Leaper, R., Hill, N. A., Edgar, G. J., Ellis, N., Lawrence, E., Pitcher, C. R., et al. (2011). Predictions of beta  
581 diversity for reef macroalgae across southeastern Australia. *Ecosphere* 2, 1–18
- 582 Lombard, A. T., Strauss, T., Harris, J., Sink, K., Attwood, C., and Hutchings, L. (2004). *South African*  
583 *National Spatial Biodiversity Assessment 2004*. Tech. rep., South African National Biodiversity Institute
- 584 Lüning, K., Yarish, C., and Kirkman, H. (1990). *Seaweeds: their environment, biogeography, and*  
585 *ecophysiology* (John Wiley & Sons)
- 586 Marlow, J. R., Lange, C. B., Wefer, G., and Rosell-Mele, A. (2000). Upwelling intensification as part of the  
587 Pliocene-Pleistocene climate transition. *Science* 290, 2288–2291
- 588 McClain, C. R., Stegen, J. C., and Hurlbert, A. H. (2011). Dispersal, environmental niches and oceanic-  
589 scale turnover in deep-sea bivalves. *Proceedings of the Royal Society of London B: Biological Sciences*,  
590 rspb20112166
- 591 Mead, A., Griffiths, C. L., Branch, G. M., McQuaid, C. D., Blamey, L. K., Bolton, J. J., et al. (2013). Human-  
592 mediated drivers of change – impacts on coastal ecosystems and marine biota of South Africa. *African*  
593 *Journal of Marine Science* 35, 403–425
- 594 Melo, A. S., Rangel, T. F. L. V. B., and Diniz-Filho, J. A. F. (2009). Environmental drivers of beta-diversity  
595 patterns in New-World birds and mammals. *Ecography* 32, 226–236
- 596 Minchin, P. R. (1987). An evaluation of the relative robustness of techniques for ecological ordination.  
597 *Vegetatio* 69, 89–107. doi:10.1007/BF00038690
- 598 Nekola, J. C., White, P. S., Carolina, N., Nekola, C., and Curriculum, P. S. W. (1999). The distance decay of  
599 similarity in biogeography and ecology. *Journal of Biogeography* 26, 867–878
- 600 Oksanen, J., Blanchet, F. G., Friendly, M., Kindt, R., Legendre, P., McGlinn, D., et al. (2016). *vegan:*  
601 *Community Ecology Package*. R package version 2.4-0
- 602 Peres-Neto, P. R. and Legendre, P. (2010). Estimating and controlling for spatial structure in the study of  
603 ecological communities. *Global Ecology and Biogeography* 19, 174–184
- 604 Peres-Neto, P. R., Legendre, P., Dray, S., and Borcard, D. (2006). Variation partitioning of species data  
605 matrices: estimation and comparison of fractions. *Ecology* 87, 2614–2625
- 606 Potts, W. M., Henriques, R., Santos, C. V., Munnik, K., Ansorge, I., Dufois, F., et al. (2014). Ocean warming,  
607 a rapid distributional shift, and the hybridization of a coastal fish species. *Global Change Biology* 20,  
608 2765–2777
- 609 Qian, H. and Ricklefs, R. E. (2007). A latitudinal gradient in large-scale beta diversity for vascular plants  
610 in North America. *Ecology Letters* 10, 737–744
- 611 R Core Team (2017). *R: A Language and Environment for Statistical Computing*. R Foundation for Statistical  
612 Computing, Vienna, Austria
- 613 Santelices, B., Bolton, J., and Meneses, I. (2009). Chapter 6. marine algal communities. *Marine*  
614 *macroecology*, 153
- 615 Schils, T. and Wilson, S. C. (2006). Temperature threshold as a biogeographic barrier in northern Indian  
616 Ocean macroalgae. *Journal of Phycology* 42, 749–756

- 617 Schlegel, R. W., Oliver, E. C. J., Wernberg, T., and Smit, A. J. (2017). Nearshore and offshore co-occurrence  
618 of marine heatwaves and cold-spells. *Progress in Oceanography* 151, 189–205
- 619 Sink, K. J., Branch, G. M., and Harris, J. M. (2005). Biogeographic patterns in rocky intertidal communities  
620 in KwaZulu-Natal, South Africa. *African Journal of Marine Science* 27, 81–96
- 621 Smale, D., Kendrick, G., and Wernberg, T. (2011). Subtidal macroalgal richness, diversity and turnover, at  
622 multiple spatial scales, along the southwestern Australian coastline. *Estuarine, Coastal and Shelf Science*  
623 91, 224–231
- 624 Smale, D. A., Kendrick, G. A., and Wernberg, T. (2010). Assemblage turnover and taxonomic sufficiency of  
625 subtidal macroalgae at multiple spatial scales. *Journal of Experimental Marine Biology and Ecology* 384,  
626 76–86
- 627 Smit, A. J., Roberts, M., Anderson, R. J., Dufois, F., Dudley, S. F. J., Bornman, T. G., et al. (2013).  
628 A coastal seawater temperature dataset for biogeographical studies: large biases between *in situ* and  
629 remotely-sensed data sets around the coast of South Africa. *PLOS ONE* 8, e81944
- 630 Soininen, J., McDonald, R., and Hillebrand, H. (2007). The distance decay of similarity in ecological  
631 communities. *Ecography* 30, 3–12
- 632 Spalding, M. D., Agostini, V. N., Rice, J., and Grant, S. M. (2012). Pelagic provinces of the world: a  
633 biogeographic classification of the world's surface pelagic waters. *Ocean and Coastal Management* 60,  
634 19–30
- 635 Spalding, M. D., Fox, H. E., Allen, G. R., Davidson, N., Ferdaña, Z. A., Finlayson, M. A. X., et al. (2007).  
636 Marine ecoregions of the world: a bioregionalization of coastal and shelf areas. *BioScience* 57, 573–583
- 637 Stegenga, H., Bolton, J. J., and Anderson, R. J. (1997). Seaweeds of the South African west coast.  
638 *Contributions of the Bolus Herbarium* 18, 3–637
- 639 Stephenson, T. A. (1948). The constitution of the intertidal fauna and flora of South Africa, Part 3. *Annals  
640 of the Natal Museum* 11, 207–324
- 641 Straub, S. C., Thomsen, M. S., and Wernberg, T. (2016). The dynamic biogeography of the anthropocene:  
642 The speed of recent range shifts in seaweeds. In *Seaweed Phylogeography* (Springer). 63–93
- 643 Stuart-Smith, R. D., Edgar, G. J., and Bates, A. E. (2017). Thermal limits to the geographic distributions of  
644 shallow-water marine species. *Nature Ecology & Evolution*, 1–9
- 645 Tittensor, D. P., Mora, C., Jetz, W., Lotze, H. K., Ricard, D., Berghe, E. V., et al. (2010). Global patterns and  
646 predictors of marine biodiversity across taxa. *Nature* 466, 1098–1101
- 647 Tonial, M., Silva, H., Tonial, I., Costa, M., Silva Júnior, N. J., and Diniz-Filho, J. (2012). Geographical  
648 patterns and partition of turnover and richness components of beta-diversity in faunas from Tocantins  
649 river valley. *Brazilian Journal of Biology* 72, 497–504
- 650 Tuya, F., Cacabelos, E., Duarte, P., Jacinto, D., Castro, J., Silva, T., et al. (2012). Patterns of landscape and  
651 assemblage structure along a latitudinal gradient in ocean climate. *Marine Ecology Progress Series* 466,  
652 9–19
- 653 Tyberghein, L., Verbruggen, H., Pauly, K., Troupin, C., Mineur, F., and De Clerck, O. (2012). Bio-  
654 ORACLE: a global environmental dataset for marine species distribution modelling. *Global Ecology  
655 and Biogeography* 21, 272–281
- 656 van den Hoek, C. (1982a). Phytogeographic distribution groups of benthic marine algae in the  
657 North Atlantic Ocean. A review of experimental evidence from life history studies. *Helgoländer  
658 Meeresuntersuchungen* 35, 153–214
- 659 van den Hoek, C. (1982b). The distribution of benthic marine algae in relation to the temperature regulation  
660 of their life histories. *Biological Journal of the Linnean Society* 18, 81–144

- 661 Verbruggen, H., Tyberghein, L., Pauly, K., Vlaeminck, C., Nieuwenhuyze, K. V., Kooistra, W. H. C. F., et al.  
662 (2009). Macroecology meets macroevolution: evolutionary niche dynamics in the seaweed *Halimeda*.  
663 *Global Ecology and Biogeography* 18, 393–405
- 664 Waldron, H. N. and Probyn, T. A. (1992). Nitrate supply and potential new production in the Benguela  
665 upwelling system. *South African Journal of Marine Science* 12, 29–39
- 666 Waters, J. M., Wernberg, T., Connell, S. D., Thomsen, M. S., Zuccarello, G. C., Kraft, G. T., et al. (2010).  
667 Australia's marine biogeography revisited: back to the future? *Austral Ecology* 35, 988–992
- 668 Wernberg, T., Thomsen, M. S., Connell, S. D., Russell, B. D., Waters, J. M., Zuccarello, G. C., et al. (2013).  
669 The footprint of continental-scale ocean currents on the biogeography of seaweeds. *PLOS ONE* 8, e80168
- 670 Whittaker, R. H. (1960). Vegetation of the Siskiyou mountains, Oregon and California. *Ecological  
671 Monographs* 30, 279–338
- 672 Whittaker, R. H. (1972). Evolution and measurement of species diversity. *Taxon*, 213–251
- 673 Wieters, E. A., Broitman, B. R., and Branch, G. M. (2009). Benthic community structure and  
674 spatiotemporal thermal regimes in two upwelling ecosystems: comparisons between South Africa and  
675 Chile. *Limnology and Oceanography* 54, 1060–1072
- 676 Zintzen, V., Anderson, M. J., Roberts, C. D., and Diebel, C. E. (2011). Increasing variation in taxonomic  
677 distinctness reveals clusters of specialists in the deep sea. *Ecography* 34, 306–317

## Tables

**Table 1.** Variance partitioning of  $\beta_{\text{sim}}$  and  $\beta_{\text{sne}}$  by the thermal and spatial predictors.  $F$  and  $p$ -values are shown for the testable fractions only.

| Fraction   |  | d.f. | Adj. $r^2$ | $F$     | $P$   |
|--|--|------|------------|---------|-------|
| <b>turnover, <math>\beta_{\text{sim}}</math></b>             |  |      |            |         |       |
| [E], thermal variables                                       |  | 4    | 0.842      | 110.160 | 0.001 |
| [S], spatial variables                                       |  | 16   | 0.961      | 80.731  | 0.001 |
| [E+S], all thermal and spatial                               |  | 20   | 0.979      | 191.560 | 0.001 |
| [E S], thermal, non-spatial                                  |  | 4    | 0.018      | 20.506  | 0.001 |
| [E with S], spatially structured thermal                     |  |      | 0.824      |         |       |
| [S E], spatial, non-thermal                                  |  | 16   | 0.137      | 23.649  | 0.001 |
| 1-[E+S], residual variance                                   |  |      | 0.021      |         |       |
| <b>nestedness-resultant, <math>\beta_{\text{sne}}</math></b> |  |      |            |         |       |
| [E], thermal variables                                       |  | 1    | 0.391      | -6.017  | —     |
| [S], spatial variables                                       |  | 4    | 0.678      | 12.060  | 0.001 |
| [E+S], all thermal and spatial                               |  | 5    | 0.714      | 9.077   | 0.001 |
| [E S], thermal, non-spatial                                  |  | 1    | 0.040      | -1.018  | 0.997 |
| [E with S], spatially structured thermal                     |  |      | 0.355      |         |       |
| [S E], spatial, non-thermal                                  |  | 4    | 0.323      | 14.277  | 0.001 |
| 1-[E+S], residual variance                                   |  |      | 0.286      |         |       |

**Table 2.**  $\beta$ -diversity ( $\beta_{\text{sor}}$ ) as well as its partitioning into  $\beta_{\text{sim}}$  and  $\beta_{\text{sne}}$  components. The partitioning represents the contribution of turnover and nestedness-resultant processes. Mean  $\pm$  SD values are presented for the whole South African coast, as well as for each of the four bioregions.

| Region  | $\beta_{\text{sor}}$ | $\beta_{\text{sim}}$ | $\beta_{\text{sne}}$ | $\beta_{\text{sne}}/\beta_{\text{sor}}$ |
|---------|----------------------|----------------------|----------------------|---|
| BMP     | $0.105 \pm 0.086$    | $0.044 \pm 0.053$    | $0.061 \pm 0.059$    | 0.581                                   |
| B-ATZ   | $0.098 \pm 0.068$    | $0.083 \pm 0.071$    | $0.014 \pm 0.009$    | 0.143                                   |
| AMP     | $0.117 \pm 0.076$    | $0.087 \pm 0.067$    | $0.030 \pm 0.020$    | 0.170                                   |
| ECTZ    | $0.259 \pm 0.157$    | $0.234 \pm 0.162$    | $0.025 \pm 0.018$    | 0.097                                   |
| overall | $0.496 \pm 0.287$    | $0.433 \pm 0.277$    | $0.063 \pm 0.061$    | 0.127                                   |

**Table 3. Linear regressions of pairwise  $\beta_{\text{sim}}$  and  $\beta_{\text{sne}}$  as a function of the geographical or thermal distance between the section pairs.** The thermal distances that best explain  $\beta_{\text{sim}}$  and  $\beta_{\text{sne}}$  were selected during the db-RDA procedure. Here,  $\beta$  is the slope of the regression line (per 100 km in the case of the relationship with distance), and the  $P$ -value test the hypothesis that the slope is significantly different from 0 using a  $t$ -test. Refer to Fig. 5a–g.

| bioregion                               | $\beta$            | $t$ -value | $P$    | Adj. $r^2$ |
|---|--------------------|------------|--------|------------|
| $\beta_{\text{sim}}$ vs. distance       |                    |            |        |            |
| BMP                                     | $0.007 \pm 0.002$  | 3.886      | <0.001 | 0.052      |
| B-ATZ                                   | $0.109 \pm 0.016$  | 6.873      | <0.001 | 0.658      |
| AMP                                     | $0.029 \pm 0.001$  | 44.751     | <0.001 | 0.834      |
| ECTZ                                    | $0.079 \pm 0.001$  | 65.003     | <0.001 | 0.936      |
| $\beta_{\text{sim}}$ vs. augMean $d_E$  |                    |            |        |            |
| BMP                                     | $0.009 \pm 0.012$  | 0.765      | 0.445  | -0.001     |
| B-ATZ                                   | $0.342 \pm 0.060$  | 6.139      | <0.001 | 0.605      |
| AMP                                     | $0.290 \pm 0.010$  | 29.209     | <0.001 | 0.681      |
| ECTZ                                    | $0.350 \pm 0.011$  | 31.200     | <0.001 | 0.772      |
| $\beta_{\text{sim}}$ vs. febRange $d_E$ |                    |            |        |            |
| BMP                                     | $0.008 \pm 0.011$  | 0.710      | 0.479  | -0.002     |
| B-ATZ                                   | $0.259 \pm 0.047$  | 5.491      | <0.001 | 0.548      |
| AMP                                     | $-0.006 \pm 0.004$ | -1.422     | 0.156  | 0.003      |
| ECTZ                                    | $0.183 \pm 0.009$  | 20.102     | <0.001 | 0.583      |
| $\beta_{\text{sim}}$ vs. febSD $d_E$    |                    |            |        |            |
| BMP                                     | $0.018 \pm 0.011$  | 1.583      | 0.115  | 0.006      |
| B-ATZ                                   | $0.161 \pm 0.080$  | 2.029      | 0.054  | 0.115      |
| AMP                                     | $-0.007 \pm 0.002$ | -2.758     | 0.006  | 0.016      |
| ECTZ                                    | $0.171 \pm 0.013$  | 13.401     | <0.001 | 0.383      |
| $\beta_{\text{sim}}$ vs. augSD $d_E$    |                    |            |        |            |
| BMP                                     | $0.038 \pm 0.008$  | 4.590      | <0.001 | 0.073      |
| B-ATZ                                   | $0.103 \pm 0.032$  | 3.183      | 0.004  | 0.276      |
| AMP                                     | $-0.003 \pm 0.003$ | -0.936     | 0.350  | 0.000      |
| ECTZ                                    | $0.082 \pm 0.008$  | 11.411     | <0.001 | 0.310      |
| $\beta_{\text{sne}}$ vs. distance       |                    |            |        |            |
| BMP                                     | $0.015 \pm 0.002$  | 8.178      | <0.001 | 0.205      |
| B-ATZ                                   | $0.006 \pm 0.004$  | 1.541      | 0.137  | 0.054      |
| AMP                                     | $0.006 \pm 0.000$  | 15.255     | <0.001 | 0.367      |
| ECTZ                                    | $-0.001 \pm 0.001$ | -2.200     | 0.029  | 0.013      |
| $\beta_{\text{sne}}$ vs. annMean $d_E$  |                    |            |        |            |
| BMP                                     | $0.067 \pm 0.009$  | 7.141      | <0.001 | 0.164      |
| B-ATZ                                   | $0.037 \pm 0.013$  | 2.929      | 0.008  | 0.240      |
| AMP                                     | $-0.009 \pm 0.004$ | -2.499     | 0.013  | 0.013      |
| ECTZ                                    | $-0.002 \pm 0.003$ | -0.845     | 0.399  | -0.001     |

## Figures and captions

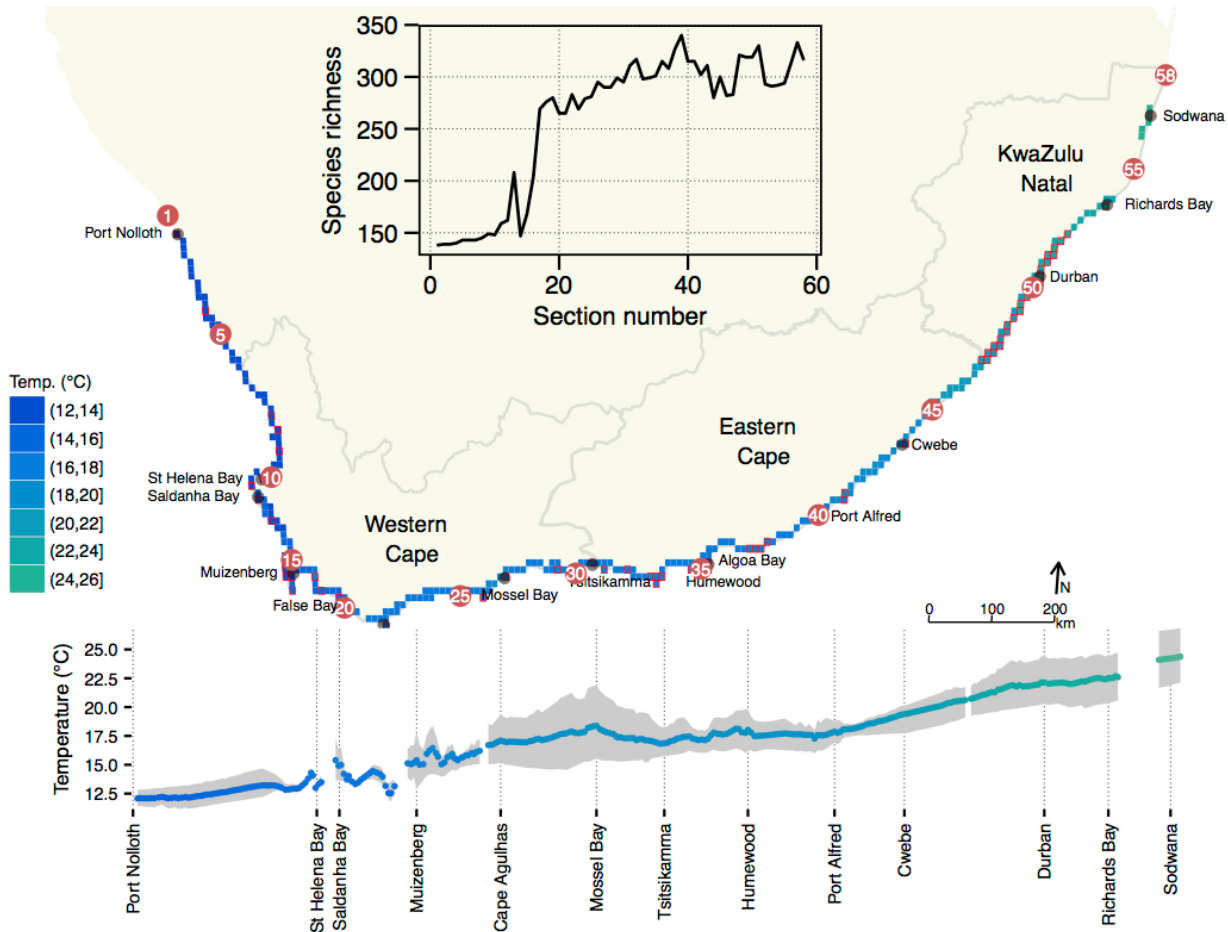


**Figure 1. Profile of mean annual temperature along the coast of South Africa.** Profiles are indicated as a function of geographical position on a coastal map (top) and as a function of distance away from Section 1 (bottom). The latter visualisation also indicates the long-term minimum (mean August) and maximum (mean February) temperatures as a grey shaded area around the annual mean temperature. The inset shows the species richness of macroalgae along the coast. Note that although a detailed temperature profile is displayed here, further analyses in this paper proceed with temperature data interpolated to the 58 sections for which seaweed diversity data are available.

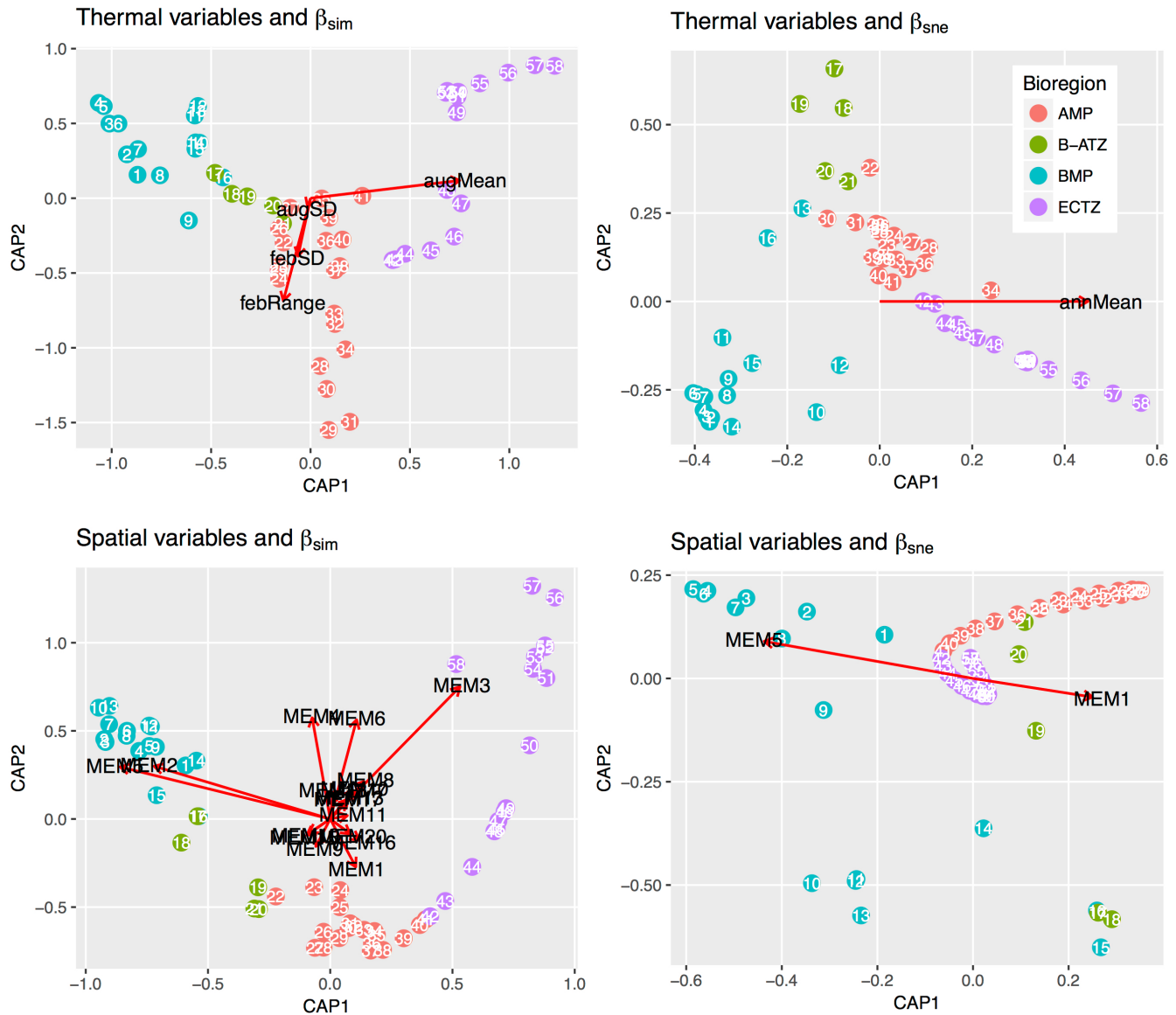


**Figure 2. db-RDA biplots of  $\text{lc}$  scores for  $\beta_{\text{sim}}$  and  $\beta_{\text{sne}}$  constrained by the thermal and spatial MEM variables.** The only two canonical axes shown are CAP1 and CAP2 since these capture the bulk of the inertia present in the ordinations. The constraining vectors were selected during the db-RDA steps.

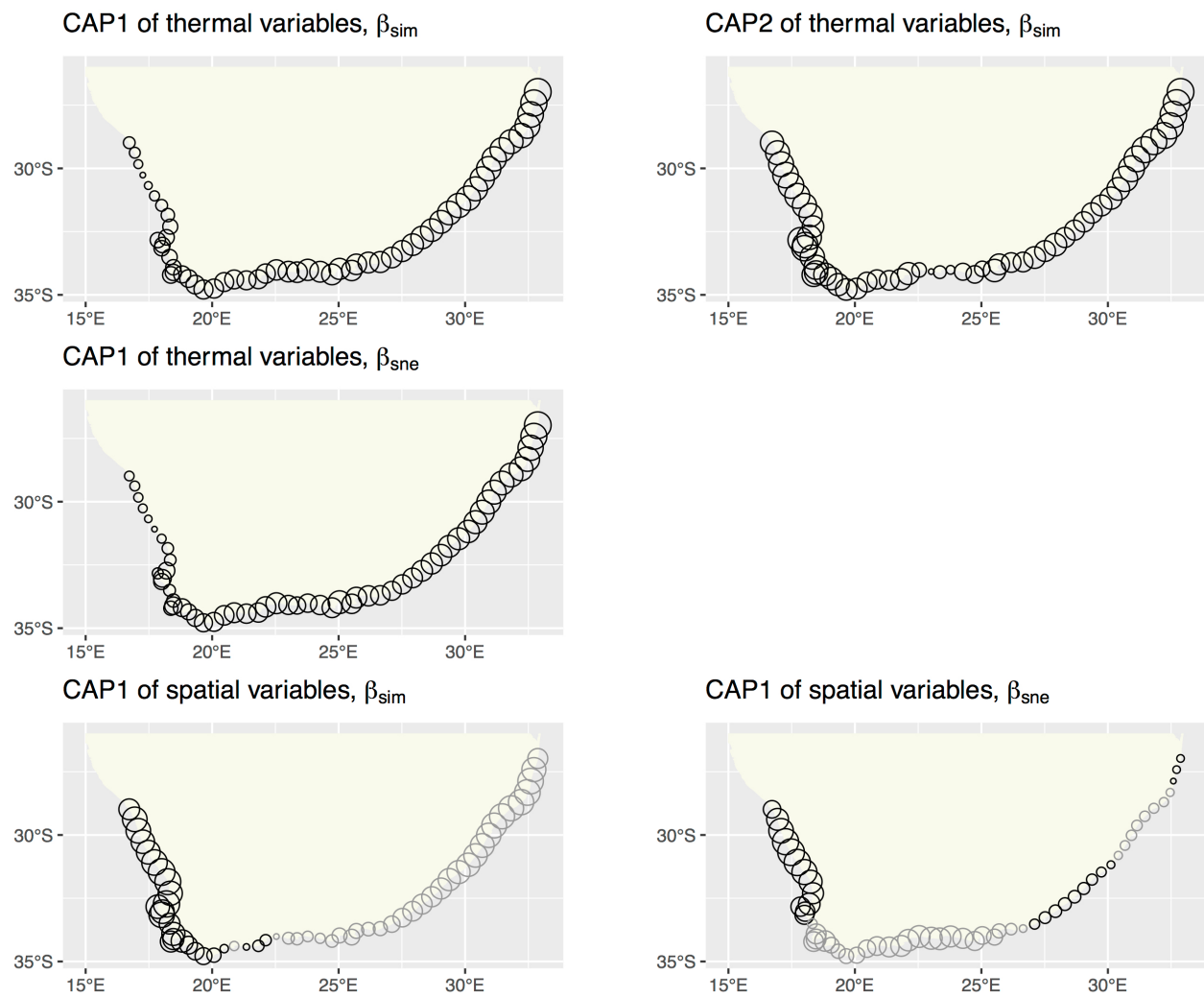


**Figure 3. db-RDA site scores for  $\beta_{\text{sim}}$  and  $\beta_{\text{sne}}$  on geographic coordinates.** The site scores indicate the major gradients captured by the environmental and spatial (MEM) constraints. Gray circles indicate negative site scores.

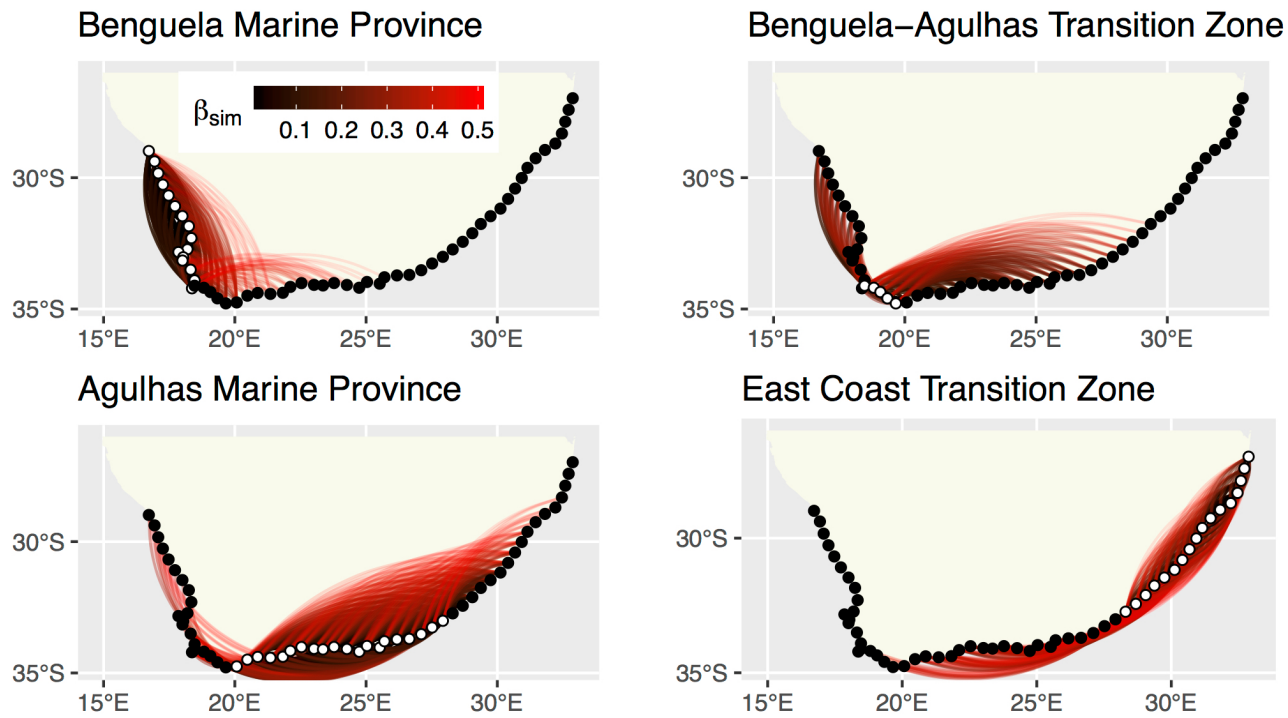


**Figure 4.** Network graphs of pairwise  $\beta_{sim}$  showing sections that are similar to one-another in species composition. Dissimilarity indices range from >0.0–0.5 (possible dissimilarities range from 0.0–1.0). The 58 sections in Appendix A appear as dots at the vertices of the network graph, with those belonging with the ‘active’ bioregion shown in white. The pairwise dissimilarities are shown by the coloured lines, with blacker lines indicating lower dissimilarity indices (species composition more similar) and redder ones higher dissimilarity indices (species composition more dissimilar).

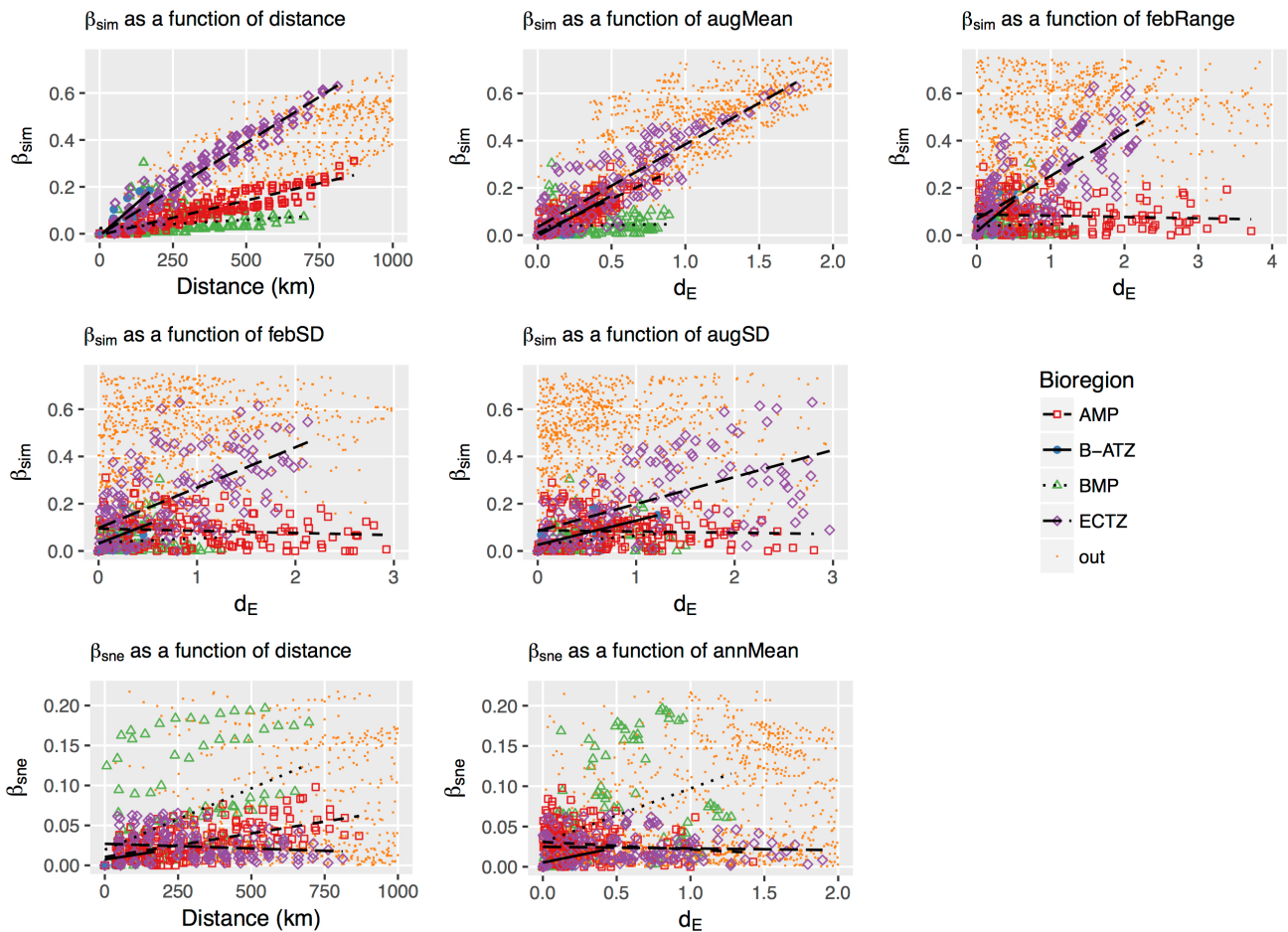


**Figure 5.** Plots of the turnover ( $\beta_{sim}$ ) and nestedness-resultant ( $\beta_{sne}$ ) forms of  $\beta$ -diversity as a function of geographical or thermal distance between the coastal sections. The influential  $d_E$  variables (*augMean*, *febRange*, *febSD* and *augSD* for  $\beta_{sim}$ , and *annMean* for  $\beta_{sne}$ ) were determined in the db-RDA procedure.  $\beta_{sim}$ ,  $\beta_{sne}$ ,  $d_E$  and geographical distance were calculated as differences between coastal section pairs, and data points representing section pairs falling between bioregions are coloured yellow and labelled 'out'. The strengths and gradients of the regression lines indicated in the panels are presented in Table 3.